Biomaterials 31 (2010) 6555–6566

Contents lists available at ScienceDirect

Biomaterials

journal homepage: www.elsevier.com/locate/biomaterials

The biocompatibility of amino functionalized CdSe/ZnS quantum-dot-Doped SiO_2 nanoparticles with primary neural cells and their gene carrying performance☆

Giuseppe Bardi [a,*], Maria Ada Malvindi [b], Lisa Gherardini [a], Mario Costa [a], Pier Paolo Pompa [b], Roberto Cingolani [b], Tommaso Pizzorusso [a,c]

[a] CNR Neuroscience Institute, Pisa, Italy
[b] Center for Bio-Molecular Nanotechnology, Italian Institute of Technology (IIT), Arnesano (Lecce), Italy
[c] Department of Psychology, University of Florence, Italy

ARTICLE INFO

Article history:
Received 10 March 2010
Accepted 29 April 2010
Available online 7 June 2010

Keywords:
Silica nanoparticles
Neural cells
Biocompatibility
Gene transfer

ABSTRACT

Nanoparticles have an enormous potential for the development of applications in biomedicine such as gene or drug delivery. We developed and characterized NH_2 functionalized CdSe/ZnS quantum dot (QD)-doped SiO_2 nanoparticles (NPs) with both imaging and gene carrier capabilities. We show that QD-doped SiO_2 NPs are internalized by primary cortical neural cells without inducing cell death *in vitro* and *in vivo*. Moreover, the ability to bind, transport and release DNA into the cell allows GFP-plasmid transfection of NIH-3T3 and human neuroblastoma SH-SY5Y cell lines. QD-doped SiO_2 NPs properties make them a valuable tool for future nanomedicine application.

1. Introduction

Nanotechnology is being increasingly used to develop nanostructured materials to improve therapies for brain damage or neurodegenerative diseases [1]. The complexity of the brain represents a major challenge for basic and applied research, despite the recent scientific advancement. The neural cells structure, morphology and physiology and their interaction show a huge diversity within the central nervous system (CNS). It is not surprising, then, the intricacy to repair brain damages induced by a broad range of pathological conditions including acute or chronic degenerative disease, insults or infections. In order to safely and appropriately interact with neurons and the other cellular components of the brain tissues, nanotechnologies must fulfill biocompatibility features [2].

A careful preparation and characterization of the physicochemical properties of nanometric engineered structures interacting with biological systems requires the highest standard of precision. The toxicity of nanoparticles in solutions or colloidal suspensions which are released in biological fluids or tissues is dependent on size, structure, shape, chemistry of their surfaces in contact with cells and, obviously, on dose [3–5].

Cellular uptake of inorganic particles, for example through the process of constitutive endocytosis, is strongly regulated by particle size [6,7] such that, depending on the diameter, nanoparticles may or may not enter the cell nucleus [8]. The chemical modification of nanoparticle surfaces, often termed as functionalization, often defines the interaction with the cell membrane. The affinity of the nanoparticle with the different components of the cell membrane triggers a cascade of events leading either to a “safe” internalization or to the disruption of the cellular physiology with fatal consequences [9].

Among the several nanoparticles, mainly developed with the final goal of gene or drug delivery, silica nanoparticles demonstrated a good degree of biocompatibility [10,11]. Silica-coated nanoparticles [12], or silica nanoparticles [10], have been demonstrated to enter the cell without affecting cell survival. These insights push research toward the development of silica nanoparticles based drug delivery systems and biosensors [13–15].

The possibility to follow nanoparticles based systems by real time imaging would increase the usefulness in nanomedicine. A promising technique is combining silica nanoparticles with quantum dot (QD) technology [16–18]. The fabrication of silica nanoparticles doped with quantum dots has been demonstrated as

☆ The activity presented in this work has been supported by the CANESTRO project of the Regione Toscana.

* Corresponding author at: Department of Psychology, University of Florence c/o CNR Neuroscience Institute, Via Moruzzi 1, 56124 Pisa, Italy. Tel.: +39 050 3153205; fax: +39 050 3153220.
E-mail address: giuseppe.bardi@in.cnr.it (G. Bardi).

0142-9612/$ – see front matter © 2010 Elsevier Ltd. All rights reserved.
doi:10.1016/j.biomaterials.2010.04.063

a successful strategy to the development of probes for targeting cell lines in suspension [19].

The investigation of silica nanoparticles interaction with primary brain cells is fascinating since the nanoparticle surface could be specifically modified for drug or gene delivery. Moreover, the nanoparticle size, charge and surface chemical modification could be designed to interact with cell membranes in specific brain pathological conditions. However, so far, no data have been shown regarding QD-doped SiO_2 NPs toxicity in brain tissues *in vivo* or in primary neural cells *in vitro*.

In this study we investigate the interaction of amino modified quantum dot (QD)-doped SiO_2 nanoparticles (NPs) with neural cells in order to develop a gene delivery system with imaging capabilities.

2. Methods and materials

2.1. Chemicals

Tetraethylorthosilicate (TEOS, 99%), Ammonium hydroxide (NH_4OH, 28–30%), 3-Aminopropyltriethoxysilane (APTS, 98%) and acetic acid (99.7%) were purchased from Sigma–Aldrich. Triton X-100 was purchased from FLUKA. Cycloexane, *n*-octanol, acetone and ethanol were purchased from J.T. Baker. Iso-Propanol was purchased from Carlo Erba reagents. All chemicals were used as received without further purification. Ultrapure grade water was used in all the experiments.

2.2. Synthesis of CdSe/ZnS QD-doped SiO_2 nanoparticles in a quaternary w/o microemulsion (type 1, 50 nm size)

The quaternary w/o microemulsion was prepared at room temperature by mixing water, an organic solvent, a surfactant (Triton X-100) and a cosurfactant (*n*-octanol). TOP/TOPO capped CdSe/ZnS core/shell QDs were prepared by following

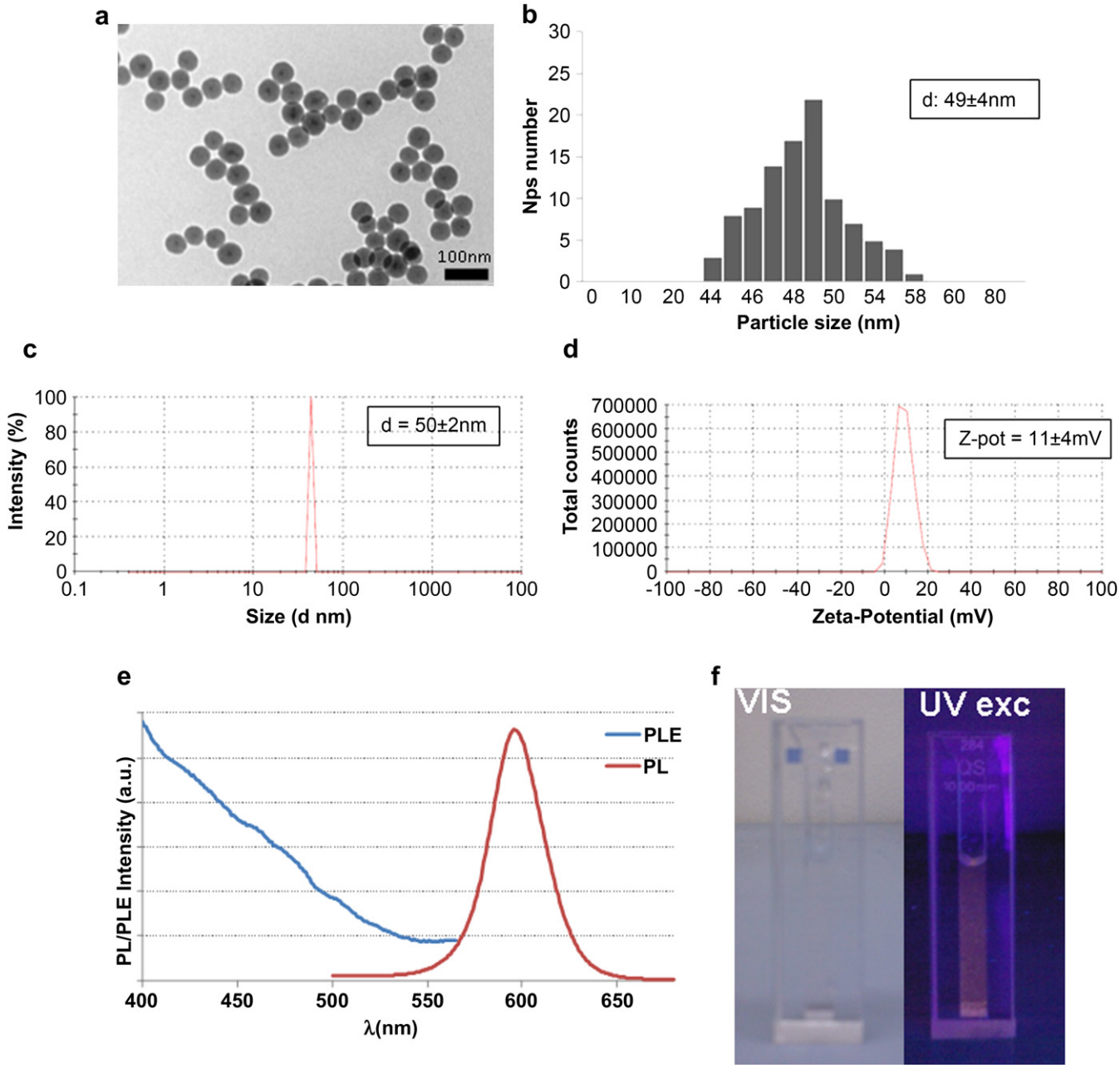

Fig. 1. *Characterization of 50 nm nanoparticles*. (a) TEM image of CdSe/ZnS QDs-doped SiO_2 NPs (50 nm); scale bar 100 nm. (b) Histogram of the particle size distribution by TEM. (c) Dynamic Light Scattering measurements. (d) Zeta-Potential measurements. (e) Spectroscopic characterization. (f) NPs suspension in water under (left) natural light and (right) UV irradiation ($\lambda_{exc} = 365$ nm).

standard colloidal synthesis procedures [20,21]. In a typical procedure, 880 μL of Triton X-100, 3.75 mL of cyclohexane, 900 μL of *n*-octanol and 1000 μmol of CdSe/ZnS QDs in chloroform (108 μM) were mixed together and stirred for 30 min. Then, 170 μL of water, 50 μL of TEOS and 30 μL of NH_4OH were added to the microemulsion. The mixture was left to stir for 24 h. After the reaction was completed, acetone was added to break the microemulsion. Nanoparticles were recovered by centrifugation (4500 rpm, 30 min, $T = 25\ ^\circ C$) and the surfactant and the unreacted molecules were washed out from the resultant precipitate of CdSe/ZnS QDs-doped SiO_2 nanoparticles sequentially, with butanol, iso-propanol, ethanol and water. The ultrasonic treatment was used to completely disperse the precipitate in the solvent and to remove the adsorbed molecules from the surface of the final product. The above mentioned conditions yielded about 15 mg of CdSe/ZnS QD-doped SiO_2 nanoparticles with 50 nm diameter.

2.3. Synthesis of CdSe/ZnS QD-doped SiO_2 nanoparticles in a ternary w/o microemulsion (type 2, 25 nm size)

The ternary microemulsion was composed of a surfactant, an organic solvent and water. 880 μL of Triton X-100, 3.75 mL of cyclohexane, 170 μL of water, 50 μL of TEOS were mixed together and stirred for 30 min. Then, 2000 μmol of CdSe/ZnS QDs in chloroform (108 μM) and 60 μL of NH_4OH were added to the microemulsion. Subsequent steps were the same as those described for the quaternary microemulsion. The above mentioned conditions yielded about 15 mg of CdSe/ZnS QD-doped SiO_2 nanoparticles with 25 nm diameter.

2.4. Preparation of amine-modified CdSe/ZnS QDs-doped SiO_2 nanoparticles

QD-doped SiO_2 nanoparticles were dispersed in freshly prepared 5% (v/v) solution of APTS and 1 mM acetic acid and stirred for 60 min. After reaction, amine-modified nanoparticles were separated by centrifugation (4500 rpm, 10 min), washed 5–6 times with acetone and water (1:1). The nanoparticles were then re-dispersed in 250 μL of water.

2.5. NH_2 functionalized CdSe/ZnS QD-doped SiO_2 nanoparticles characterization

Transmission electron microscope (TEM) images were recorded by a JEOL Jem 1011 microscope operating at an accelerating voltage of 100 kV. TEM samples were prepared by dropping a dilute solution of nanoparticles in water on carbon-coated copper grids (Formvar/Carbon 300 Mesh Cu).

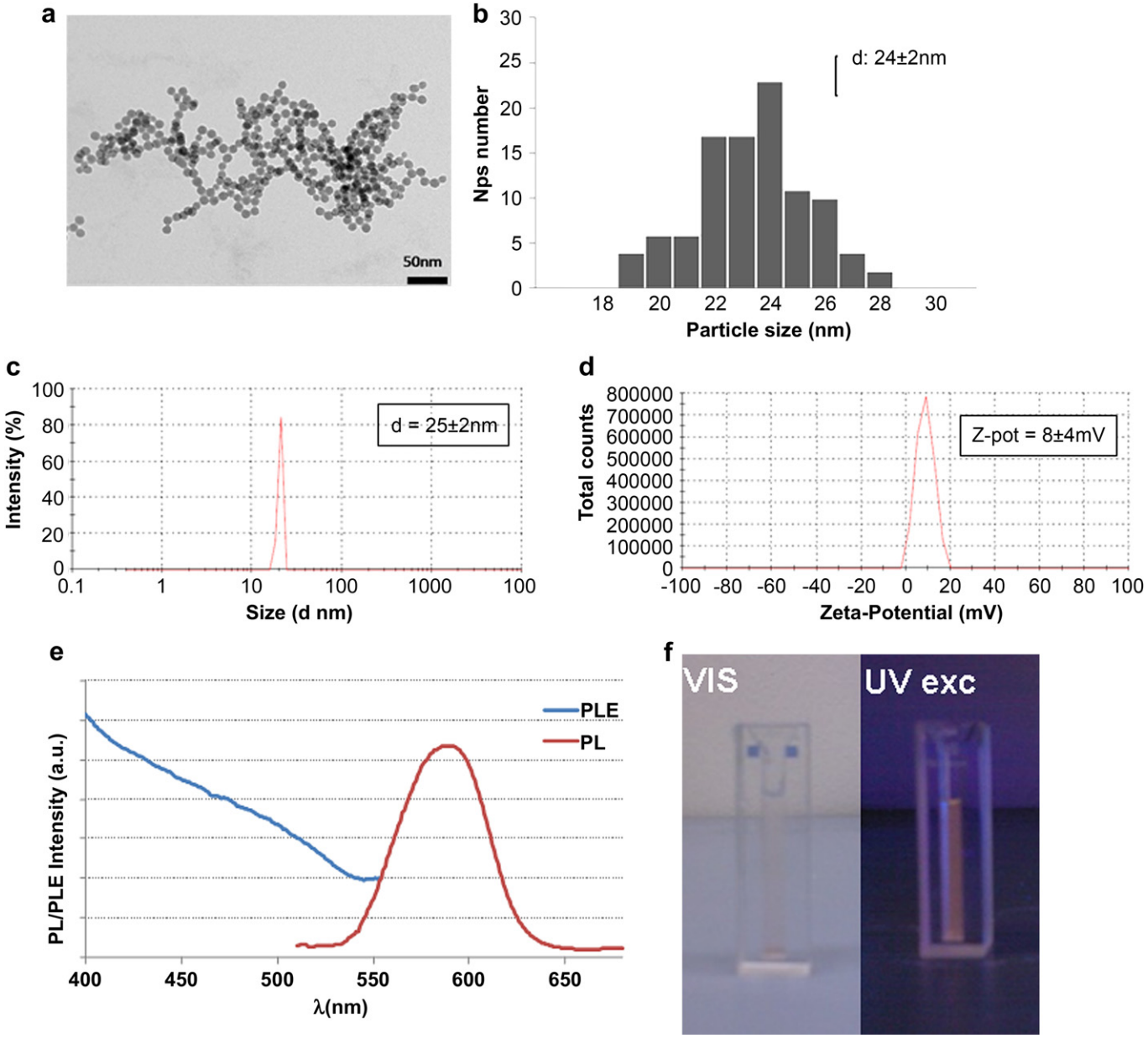

Fig. 2. *Characterization of 25 nm nanoparticles.* (a) TEM image of CdSe/ZnS QDs-doped SiO_2 NPs (25 nm); scale bar 50 nm. (b) Histogram of the particle size distribution by TEM. (c) Dynamic Light Scattering measurements. (d) Zeta-Potential measurements. (e) Spectroscopic characterization. (f) NPs suspension in water under (left) natural light and (right) UV irradiation ($\lambda_{exc} = 365$ nm).

Dynamic Light Scattering (DLS) and Zeta-Potential measurements were performed on a Zetasizer Nano ZS90 (Malvern, USA) equipped with a 4.0 mW He–Ne laser operating at 633 nm and an avalanche photodiode detector. Measurements were made at 25 °C in aqueous solutions (pH = 7).

Photoluminescence/Photoluminescence excitation (PL/PLE) measurements of NPs were recorded in photon counting mode by using a 450 W xenon lamp as the source of excitation and double monochromators both in excitation and emission. The emitted light was collected at right angles to the excitation radiation; excitation and emission bandwidths were 2 nm. Experiments were performed at room temperature (20 °C).

2.6. Photoluminescence quantum yield measurements

UV–vis absorption spectra were recorded using a Varian Cary 300 spectrophotometer while fluorescence spectra were collected by a Jobin Yvon FluoroLog-3 spectrofluorometer. Photoluminescence quantum yield (QY) measurements were performed adopting the gradient method and using Rhodamine 6 G as reference fluorescent dye (excitation wavelength at 488 nm, QY 95%).

2.7. Cell cultures

Primary mouse cortical cultures were prepared as following: brains were removed from mice at postnatal days 0–2 and placed in HBSS. Cortices were dissected and meninges removed. Chopped small pieces of cortex were triturated with a Pasteur pipette in presence of 0.25% Trypsine and DNAse to reach a single-cell suspension. After 5–10 min a small volume of suspension at the top was placed in equal volume of DMEM supplemented with 10% horse serum. Cell were then counted and directly cultured on coverslips or Petri dishes previously coated with 100 μg/ml polylysine. After 2 h DMEM/horse serum was replaced with Neurobasal-A medium supplemented with B27, 2 mM glutamine and gentamicine. After 7 days fully differentiated neurons lay on glia cells growing in a layer underneath the neurons.

NIH3T3 cell line was cultured according to ATCC indications at 37 °C 5% CO_2 in DMEM supplemented with 50 U/mL penicillin, 50 mg/mL streptomycin and 2 mM glutamine. Medium was replaced every 3 days.

SH-SY5Y human neuroblastoma cells were obtained from ATCC and cultured according to ATCC indications at 37 °C 5% CO_2 in 45% minimum essential medium, 45% Ham's F-12 medium, 10% fetal bovine serum (FBS) containing 50 μg/ml gentamycin. Medium was replaced every 3 days.

2.8. Transfection

The cells were serum starved for 2 h in presence of QD-doped SiO_2 NPs/GFP-DNA mix (10 μg/mL NPs mixed with 1 μg plasmid DNA) in a glass chamber (WillCo Wells BV, Amsterdam, Netherlands) for the Leica confocal microscope. After serum starvation DMEM without serum was replaced by complete medium supplemented with 10% FBS. Cells were left undisturbed for 24 h before confocal microscopy investigation of GFP expressing cells. All experiments have been performed at 37 °C without cell fixation.

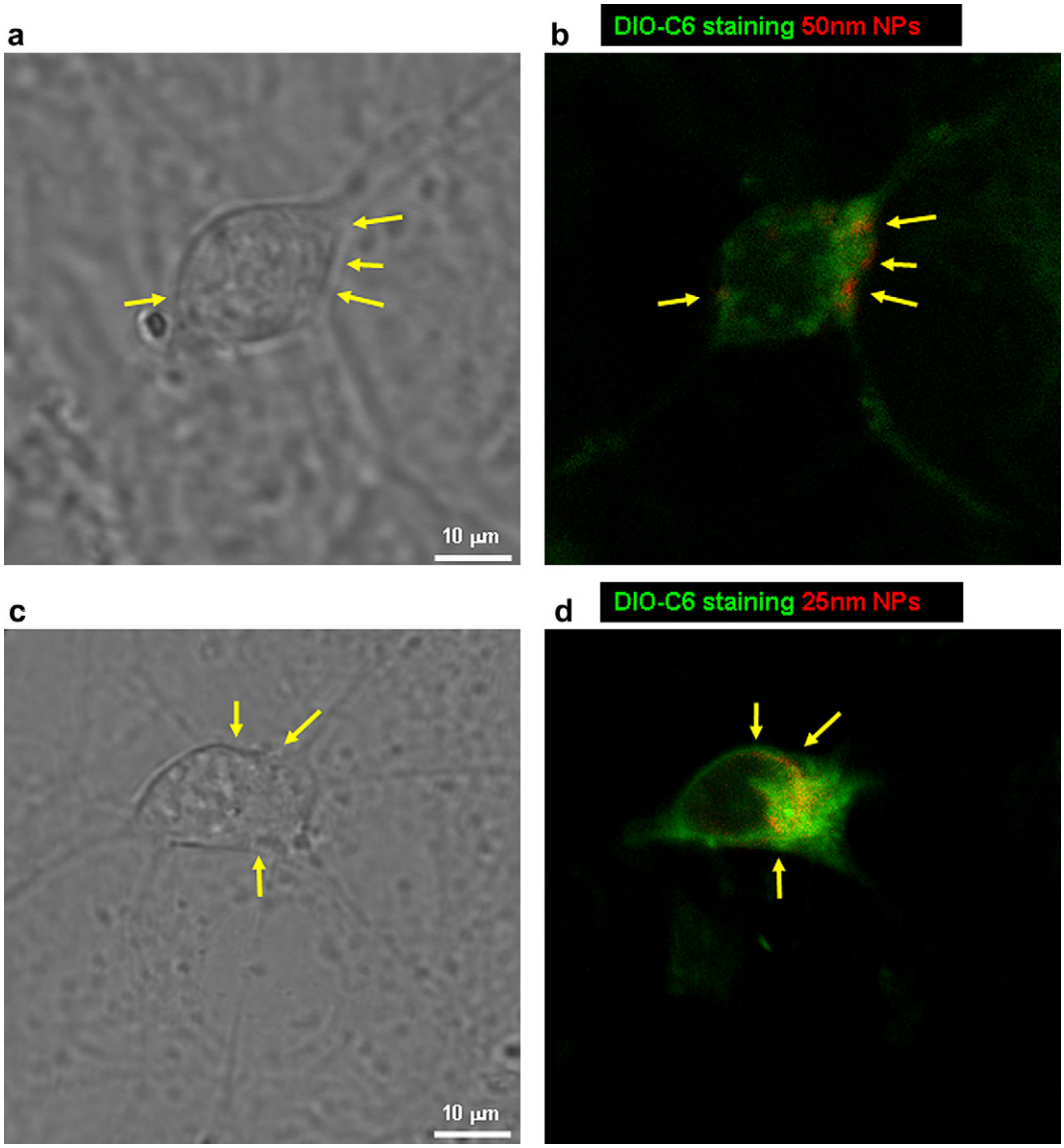

Fig. 3. *CdSe/ZnS* QDs-doped *SiO_2 NPs localization*. (a, c) Confocal microscope images of primary neurons; DIO-C6 stained neuron membranes (green) and (b) 50 nm red fluorescence emitting CdSe/ZnS QDs-doped SiO_2 NPs or (d) 25 nm CdSe/ZnS QDs-doped SiO2 NPs. Pictures have been taken after 30 min of living cell exposure to nanoparticles.

2.9. Apoptosis assays and in vitro microscopy

Fluorescence and phase contrast pictures of primary mixed cortical cultures taken without or with increasing concentration of 50 nm and 25 nm QD-doped SiO_2 NPs (from 0.1 μg/mL to 10 μg/mL). 0.5 μg/mL Hoechst 33258 nuclei staining, 5 nM DiO-C6 (Sigma–Aldrich, St. Louis, MO, USA) membrane staining (30 min, RT, dark) and phase contrast cell morphology were used to evaluate differences between normal and apoptotic cells after treatments. Phase contrast and fluorescence cell images were acquired by a camera mounted Zeiss Axioskop microscope and by Leica TCS-NT Confocal Microscope.

2.10. In vivo intracerebral injection, apoptosis and microscopy

Animals were used in accordance with protocols approved by the Italian Minister for Scientific Research. Mice were anesthetized with avertin (0.5 mL/100 g) and mounted on a stereotaxic apparatus. Injections were made at specific stereotaxic locations in the visual cortex by means of a glass pipette (30-μm tip diameter) mounted on a motorized (0.1-μm step) three-axis micromanipulator connected to an injector (Sutter Instruments, Novato, CA, USA). A total of 350 nL were released at 700 μm and another 350 nL were released 400 μm below the cortical surface to allow homogeneous dispersion of NPs along the cortical depth. During injections, animals were oxygenated and heated by means of a blanket with a thermostat to ensure a 37 °C rectal temperature. After surgery, the antibiotic gentamicin was topically administered to prevent infections. In these conditions, the whole procedure requires about 20 min, and recovery from anesthesia occurs after 60 to 90 min. After recovery, animals were returned to their home cages. Injected mice were transcardially perfused with ice-cold 4% paraformaldehyde in 0.1 M TBS and 1 mM sodium orthovanadate, pH 7.4 (TBSV). Brains were quickly removed and cryoprotected in 30% sucrose overnight and then 50 μm coronal sections were cut on cryostat and processed for apoptosis tests. To detect apoptosis we used two methods: 0.5 μg/ml

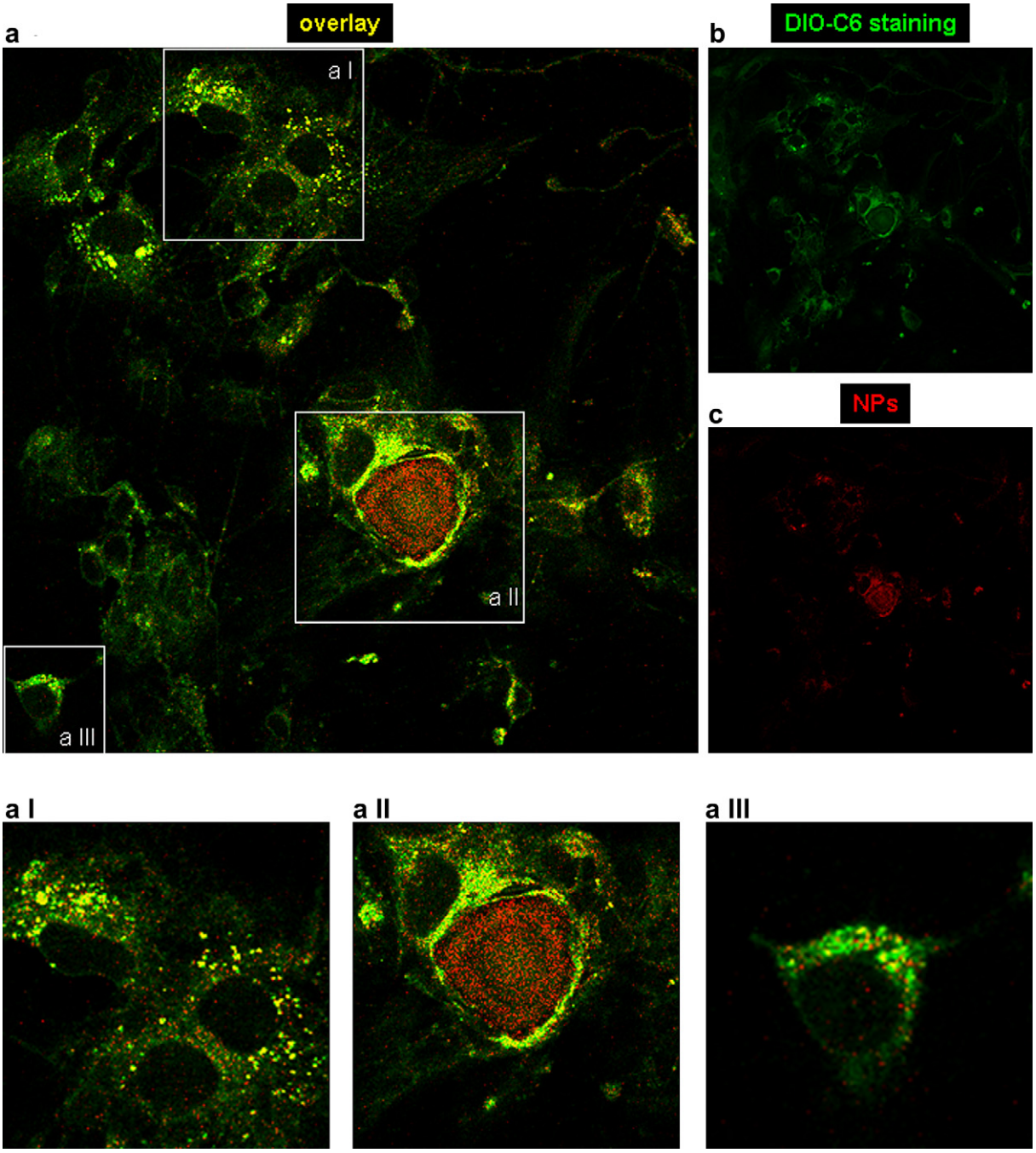

Fig. 4. *CdSe/ZnS* QDs-doped *SiO_2 NPs cell internalization*. a) 63× magnification field of a representative primary neural cell culture treated with 50 nm NPs for 24 h. The yellow color of the membranes is the result of superimposed green emission (500) of the DIO-C6 (b) staining and the red emission (590 nm) of the NPs (c). a I) particular of intracellular vesicles (yellow); a II) particular of a glia cell endosome full of NPs; a III) particular of a neuron cell body.

Hoechst 33 258 nuclei staining of fixed brain tissues and ApoAlert DNA Fragmentation Assay Kit (Clonetech Laboratories, Inc., Mountain View, Ca, USA), a fluorescence kit based on terminal deoxynucleotidyl transferase (TdT)-mediated dUTp nick-end-labeling (TUNEL). Briefly, free-floating paraformaldehyde fixed 50 μm coronal sections were treated for 5 min at room temperature (RT) with 20 μg/mL Proteinase K solution. After washing with phosphate buffered saline (PBS) solution (0.1 M) the slices were equilibrated with Equilibration Buffer at RT for 10 min. TdT incubation buffer was prepared following the Kit User Manual suggested ratios of Equilibration Buffer, Nucleotide Mix, and TdT Enzyme. The tailing reaction was performed in the dark and humidified 37 °C incubator for 60 min. The reaction was terminated by adding 2x SSC and incubating for 15 min at RT in the dark. The slices were washed with PBS before mounting on microscope slides. Slices were mounted on glass slides with Vectashield (H1000; Vector Laboratories), preparations were coverslipped, sealed with nail polish, and scanned with a Leica TCS-NT confocal microscope (Leica Microsystems) equipped with an argon–krypton laser. Apoptotic cells exhibit nuclear green fluorescence using fluorescein filter set (520 ± 20 nm).

2.11. DNA binding experiment

NH_2 functionalized CdSe/ZnS QD-doped SiO_2 NPs/DNA binding and release was investigated mixing 200 μg of 50 nm and 25 nm NPs with growing amount of plasmidic DNA. After incubation for 30 min at room temperature, 20 μL of the reaction mixture of NPs/DNA was loaded on a 1% non-denaturing agarose gel in buffer containing 45 mM Tris, 45 mM boric acid and 1 mM EDTA and ethidium bromide. After 40 min (100 V) electrophoresis, the gel has been exposed on UV transilluminator and the DNA quantified by chemiDoc analyzer biorad (Plasmid pEGFPC1 clontech).

2.12. Statistics

To evaluate the statistical significance of all the described *in vitro* experiments ten microscopic fields per coverslip were counted and three coverslips/treatments were used for each experiment. Three independent experiments have been performed in triplicate. One way statistical analysis of variance (ANOVA) followed by analysis Student-Newman-Keuls method has been performed.

3. Results and discussion

3.1. Characterization of NH_2 functionalized CdSe/ZnS QD-doped SiO_2 nanoparticles

The size of the first type of NPs (Fig. 1a, b) was found to be 49 ± 4 nm after measuring the size of more than 100 particles by TEM (Fig. 1b). On the other hand, type 2 NPs (Fig. 2a, b) was found to be 24 ± 2 nm.

Dynamic Light Scattering (DLS) determined sizes of NPs resulted in good agreement with TEM data. In fact, type 1 NPs displayed a hydrodynamic diameter of 50 ± 2 nm (Fig. 1c), while type 2 NPs were 25 ± 2 nm (Fig. 2c). After amino functionalization, 50 nm nanoparticles show a Zeta potential of +11 ± 4 mV (Fig. 1d), while 25 nm NPs of +8 ± 4 mV (Fig. 2d).

Photoluminescence/Photoluminescence excitation (PL/PLE) spectra of NPs show that the emission peak is centered around 590 nm for both 50 nm (Fig. 1e) and 25 nm NPs (Fig. 2e).

The QY of the as-synthesized QDs in chloroform was estimated to be 17%. Encapsulation of QDs in silica nanoparticles reduced the QY to 5% in both types of QD-doped NPs. However, the large extinction coefficient of QDs along with their high photostability allowed efficient and sensitive tracking of silica NPs in all the imaging experiments.

3.2. Cell internalization of NH_2 functionalized CdSe/ZnS QD-doped SiO_2 NPs

10 μg/mL of NH_2 functionalized 50 nm and 25 nm QD-doped SiO_2 NPs suspensions were administrated to the primary neural cell

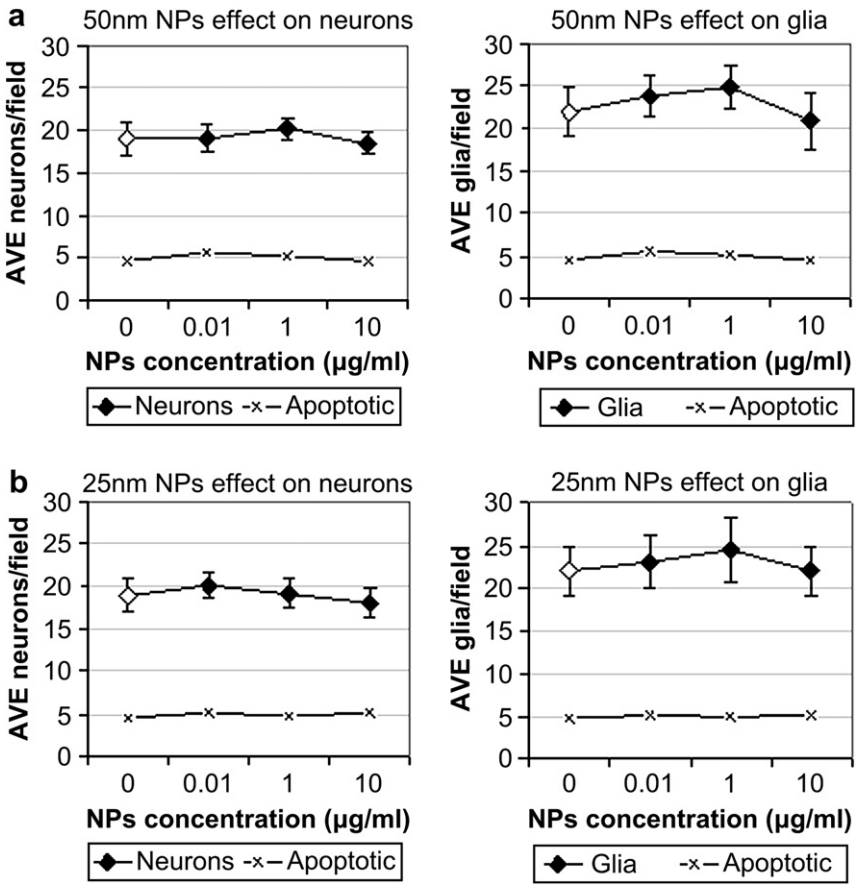

Fig. 5. *CdSe/ZnS* QDs-doped *SiO_2 NPs in vitro toxicity*. Quantification of cell number and apoptotic nuclei after 24 h at 37 °C in presence or absence of increasing concentration of SiO_2 NPs 50 nm and 25 nm (from 0.1 μg/ml to 10 μg/ml). Graphs show the number of living neurons (diamonds) or glia (diamonds) after 24 h of 50 nm and 25 nm NPs. Numbers of apoptotic cells present in the cultures shown by –x- graphs.

cultures and confocal microscopy pictures were taken. Cells were labeled with DIO-C6, a specific stain for cell membranes. Fig. 3 shows QD-doped NPs (50 nm in Fig. 3a,b; 25 nm in Fig. 3c,d) co-localizing with the external membrane of the cell body. Soon after their administration, most of the NPs can be found close to the cells (Supplementary Fig. 3, 15 min). Most likely, this is the result of the interaction between the positively charged NP surfaces and the negatively charged cell membrane.

24 h after administration of SiO_2 NPs to primary neural cultures, we could clearly observe cell internalization in both neurons and glia (Fig. 4a). A confocal microscopy analysis of QD-doped SiO_2 NPs treated cells stained with DIO-C6 specific membrane labeling (Fig. 4a and b) indicates the colocalization of NPs with cytoplasm vesicles (Fig. 4a I, yellow colored). Fig. 4a II shows a huge endosome full of NPs within a glia cell, whereas Fig. 4a III points out a neuron cell body characterized by a small cytoplasm surrounding the

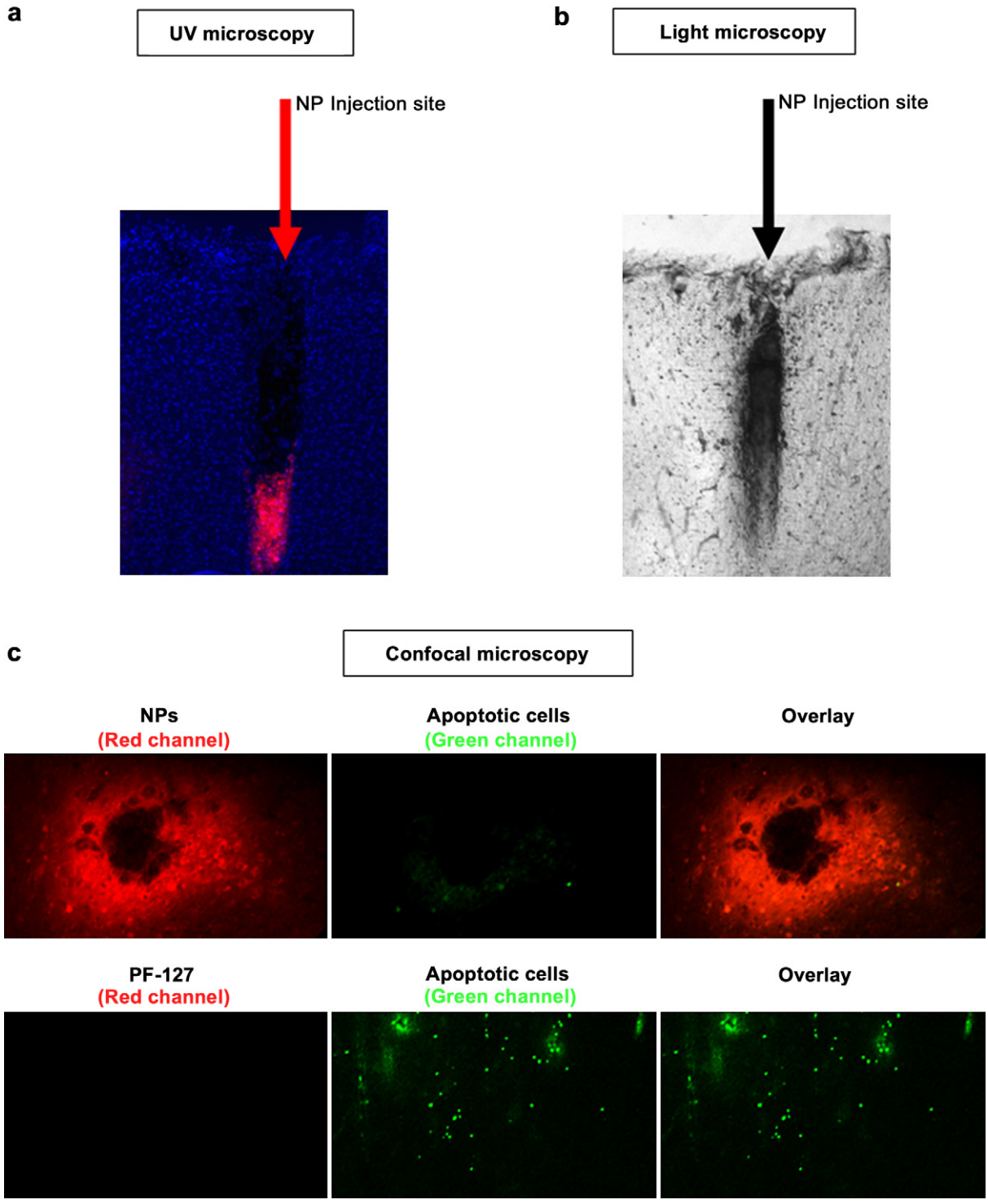

Fig. 6. *CdSe/ZnS* QDs-doped *SiO_2 NPs in vivo toxicity.* a) UV microscopy brain cortex tissue injected with 10 mg/ml 25 nm; cell nuclei stained with Hoechst 33258 (blue) b) Light microscopy picture at 10× magnification of fixed brain cortex tissue injected with 10 mg/ml 25 nm NPs. Confocal microscopy pictures of TUNEL assay treated fixed brain cortex tissue injected with 10 mg/ml 50 nm NPs (upper panel) or 5% Pluronic F-127 (lower panel).

nucleus (dark). Either glia cells or neurons can internalize NH_2 functionalized QD-doped SiO_2 NPs and most NPs could be seen in intracellular vesicles after 24 h.

The imaging capabilities of the QDs combined with cell membrane staining give us the possibility to see how the amino functionalization induce NPs colocalization with cell membrane (Fig. 3), and cell internalization (Fig. 4). The presence of most of NPs in vesicles (Fig. 4 aI) tempts us to assume the entrance through endocytosis. Not all the NPs seem to be inside the vesicles; however, the particular of Fig. 4 aII shows a big glial cell engulfing an enormous amount of NPs in a huge endosome. Fig. 4 aIII, demonstrates the presence of vesicles within a neuron body cytoplasm. So, all primary neural cells can internalize NH_2 functionalized QD-doped SiO_2 NPs engulfing most of them in the cytoplasm vesicles.

3.3. 50 nm and 25 nm NPs are non-cytotoxic for neural cells in vitro and in vivo

The presence of 50 nm or 25 nm SiO_2 NPs did not decrease the number of viable cells in culture over the 24 h following exposure (Fig. 5 and Supplementary Fig. 1). We evaluated the number of

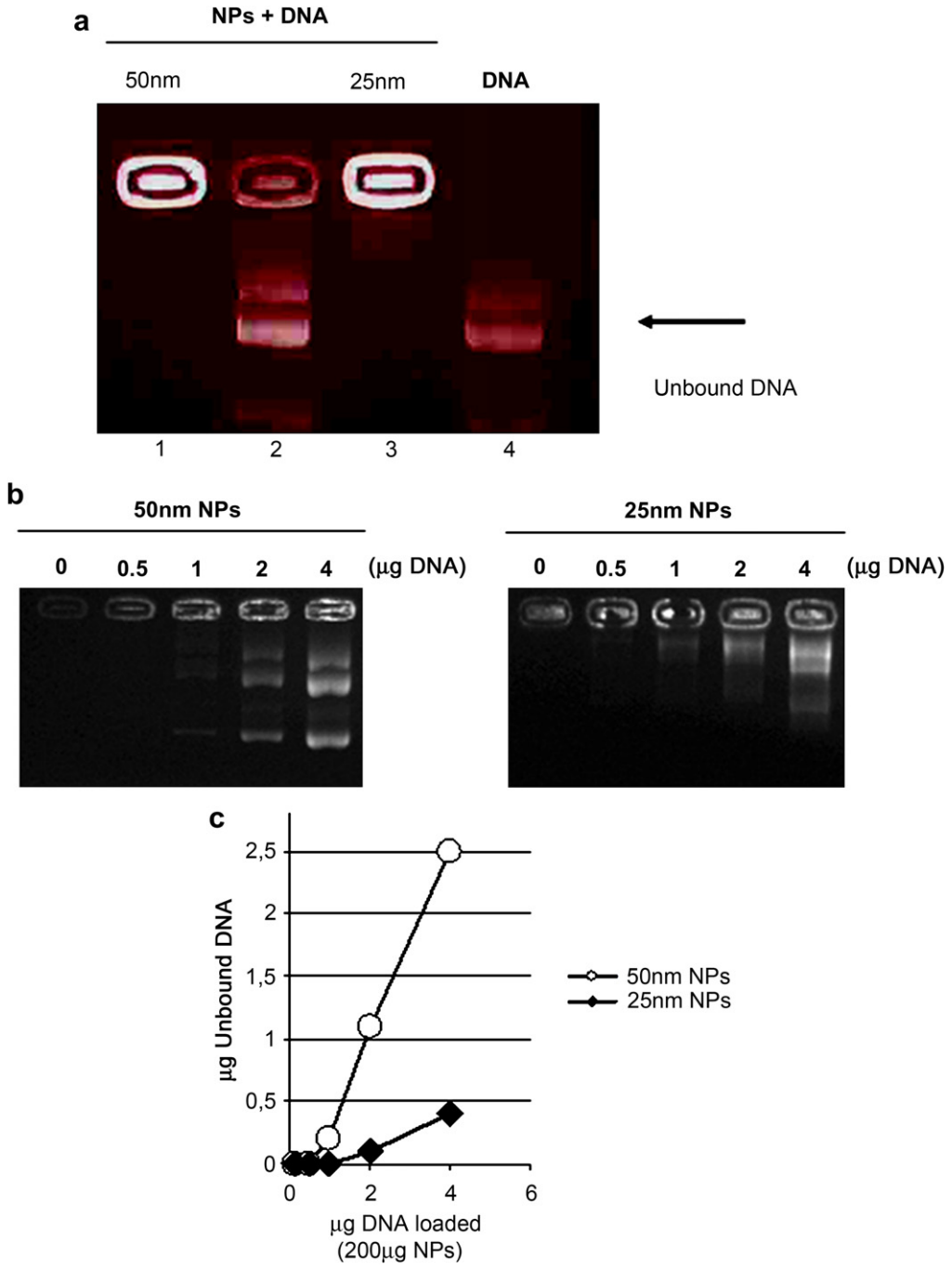

Fig. 7. *CdSe/ZnS* QDs-doped *SiO_2 NPs binding of DNA.* a) 200 µg of three different types of NPs have been mixed for 15 min at RT with 0.5 µg of plasmid DNA and loaded on an agarose gel. Columns 1 and 3, 50 nm and 25 nm NPs respectively. Column 2, a different type of NPs unable to bind DNA. Column 4, plasmid DNA alone. b) Gels showing increasing concentrations of plasmid DNA (from 0.5 to 4 µg) mixed with 200 µg of 50 nm (left panel) and 25 nm NPs (right panel) after 40 min (100 V) electrophoresis. c) Quantification by chemiDoc analyzer of the amount of DNA unbound in the different columns of the gels shown in b).

apoptotic nuclei by Hoechst staining and the neuron or glia morphology [22]. Neither 50 nm NPs (Fig. 5a) nor 25 nm NPs (Fig. 5b) in a range of concentration between 0.1 and 10 μg/ml affected neuron or glia cell viability. Primary mouse cortical or hippocampal neurons are particularly sensitive cells which can easily die as a consequence of slight alterations of their culturing conditions [23]. The concentration range of NPs chosen for the *in vitro* experiments was based on previous literature of similar silica nanoparticles tested on cell lines [11,24]. Our results are the first data available on NH_2 functionalized QD-doped SiO_2 NPs tested on primary neural cells.

To further investigate the non-cytotoxic properties of our NH_2 functionalized SiO_2 NPs *in vivo*, we delivered the colloidal NPs suspension directly into the parenchyma of living mouse brain. Brain cortex of anesthetized mice was injected with 10 mg/ml 50 nm and 25 nm QD-doped SiO_2 NPs. To allow dispersion into the dense matrix of the cerebral tissue we decided to use a higher NPs concentration with respect to the *in vitro* investigation where the mobility of the particles is facilitated by the aqueous culturing medium. Representative UV light excited Hoechst nuclei staining (Fig. 6a) and light microscopy picture (Fig. 6b) of brain cortex tissue injected with 10 mg/ml 25 nm are shown. We used a fluorescence kit based on terminal deoxynucleotidyl transferase (TdT)-mediated dUTp nick-end-labeling (TUNEL; see Method and Materials) were apoptotic nuclei appear green, to precisely evaluate the induced apoptosis *in vivo* by confocal microscopy after 3 days from the injection, Fig. 6c presents a QD-doped SiO_2 NPs injection (upper panel) and 5% Pluronic F-127 induced apoptosis as positive control (lower panel, [22]). Clearly, NPs treated tissue shows very few apoptotic cells, despite NPs relative ability to diffuse in the tissue, as indicated by the high number of bright red labeled cells surrounding the site of injection.

Our *in vivo* results (Fig. 6) demonstrate that a direct administration of amino functionalized QD-doped SiO_2 NPs into the brain do not damage the tissue structure (Fig. 6a and b) neither induce apoptotic cell death (Fig. 6d). Nevertheless, 3 days after the injection we could observe a certain degree of penetration in the surrounding tissue. We speculate that NPs dispersion into the brain tissue is probably due to cell membrane endocytosis and vesicle mediated exocytosis, as suggested by *in vitro* intracellular localization (Fig. 4).

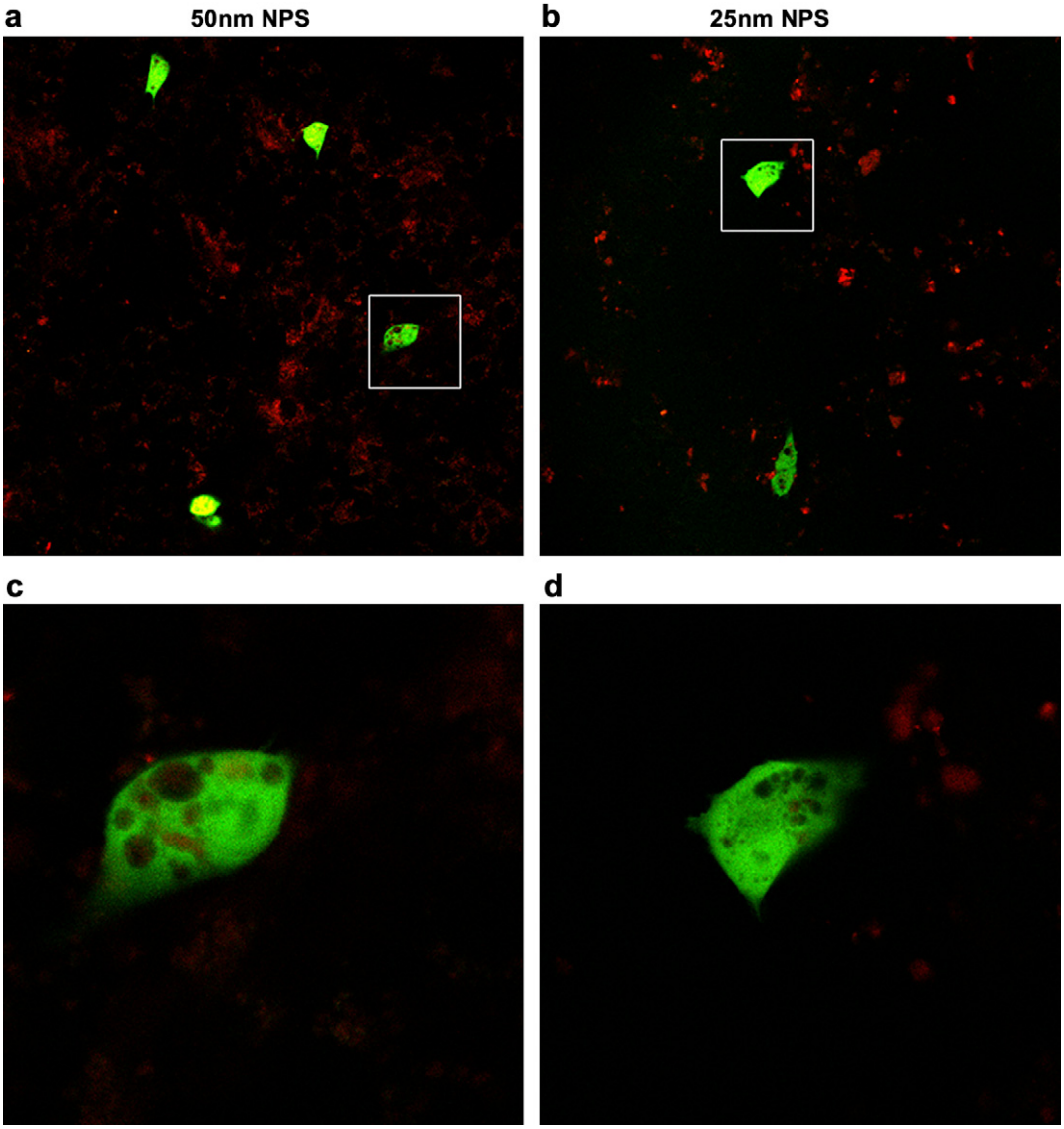

Fig. 8. QDs-doped *SiO_2 NPs mediated transfection of NIH-3T3 cell line*. a) NIH-3T3 cells expressing GFP protein (green) 24 h after exposure to 50 nm NPs (red) loaded with GFP-plasmid DNA. b) NIH-3T3 cells expressing GFP protein (green) 24 h after exposure to 25 nm NPs (red) loaded with GFP-plasmid DNA. c) and d) particular of a) and b) respectively.

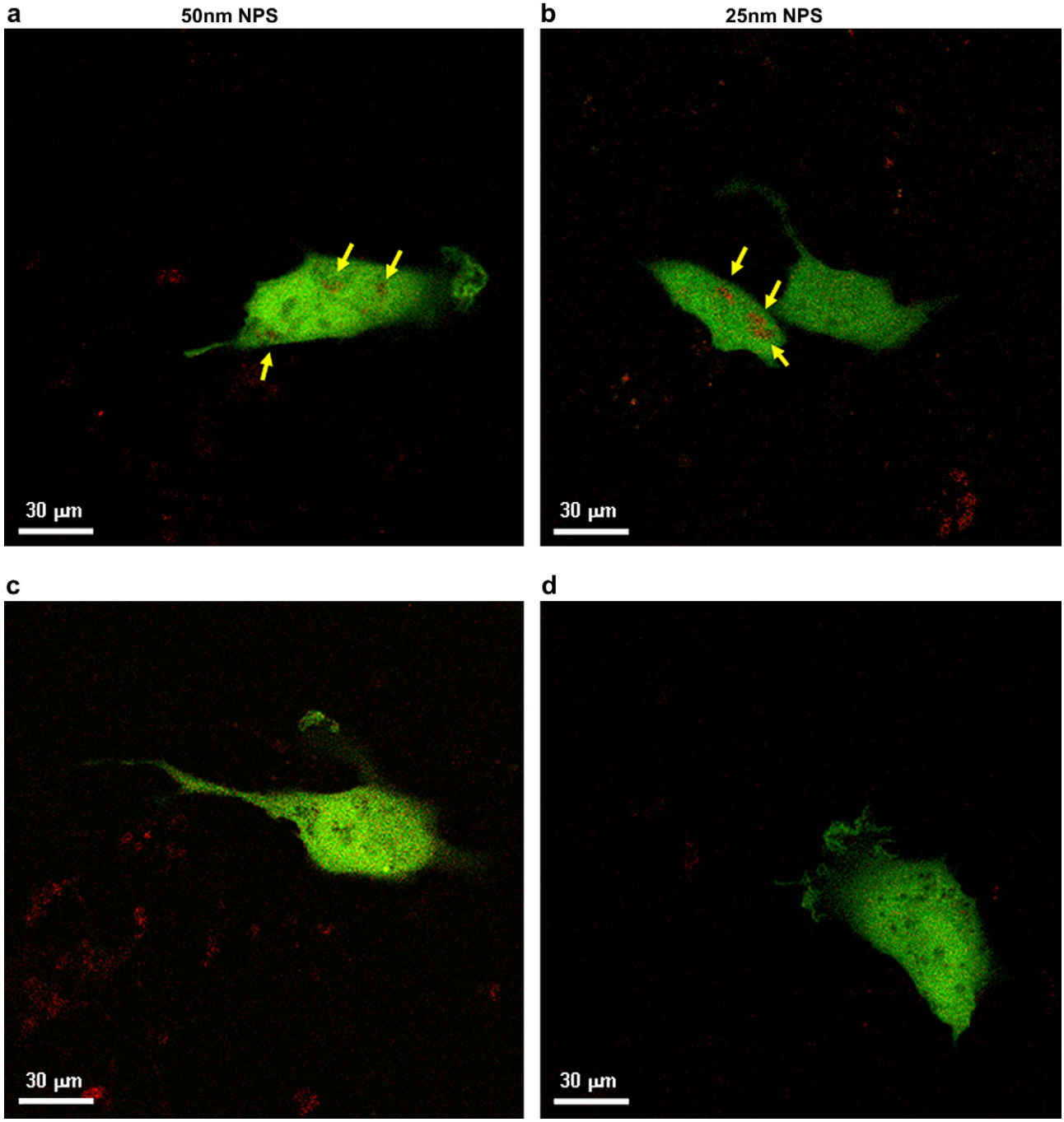

Fig. 9. QDs-doped SiO_2 NPs mediated transfection of human neuroblastoma SH-SY5Y cell line. a) and c) SH-SY5Y cells expressing GFP protein (green) 24 h after exposure to 50 nm NPs (red) loaded with GFP-plasmid. b) and d) SH-SY5Y cells expressing GFP protein (green) 24 h after exposure to 25 nm NPs (red) loaded with GFP-plasmid DNA. Yellow arrows in a) and b) show the NPs localized within the SH-SY5Y cells.

3.4. NH_2 functionalized QD-doped SiO_2 NPs can bind DNA

50 nm and 25 nm NPs have been functionalized with amine groups on the surface. This modification is responsible for their DNA binding capability as demonstrated by the electrophoresis gel pictures of Fig. 7. 50 nm and 25 nm NPs have been mixed with DNA at RT and loaded in agarose gel (column 1 and 3, respectively, Fig. 7a). After 40 min only free DNA migrated into the gel (Fig. 7a column 4), when conversely migration of DNA bound to the NPs was not detected. In column 2, DNA mixed with a different type of NPs of the same size of the 50 nm NPs but unable to bind DNA is shown as negative control.

To quantify the DNA binding capability of the amino functionalized NPs, 200 μg of 50 nm and 25 nm were allowed to bind with increasing amount of DNA (from 0 to 4 μg) and loaded on agarose gel. After 40 min of electrophoresis at 100 V, thicker bands of unbound DNA can be seen in the columns where the ratio DNA/NPs is higher (Fig. 7b). DNA bands were quantified by chemiDoc analyzer and, from the results shown in Fig. 7c graph, we estimated that 2.5 ng DNA/μg of 50 nm NPs and 5 ng DNA/μg

of 25 nm NPs can be carried by amino functionalized QD-doped SiO_2 nanoparticles.

3.5. 50 nm and 25 nm QD-doped SiO_2 NPs can transfect cells

As shown in Fig. 7 50 nm and 25 nm NPs bind DNA when mixed in solution. Moreover, the NP amino surfaces allow them to stick on the negatively charged cell membrane and to be internalized by the cells (Figs. 3 and 4). We therefore investigated whether such NPs features could be used to carry exogenous DNA through the cell membrane, to be expressed into the cells. We performed an experiment in which GFP-plasmid DNA/NPs complex was added to cells left for 2 h in serum free medium in order to avoid interaction of DNA/NPs complexes with serum proteins and facilitate binding to the cell membrane. We used NIH-3T3 cell line and human neuroblastoma SH-SY5Y cell line to investigate NPs transfection properties as these cells well survive in serum free medium for a long period. On the contrary, primary neurons would start an apoptotic pathway in serum deprived culturing conditions longer than 1 h Fig. 8 panels show fluorescence confocal pictures of NIH-3T3 24 h after DNA/NPs complexes administration. In Fig. 8a and b are visible the bright red 50 nm and 25 nm NPs defining the cell profiles and some bright green GFP expressing NIH-3T3 cells. Fig. 8c and d show the particular of a 50 nm and 25 nm NPs transfected cells, respectively. Moreover, in Fig. 9 we present that our QD-doped silica NPs were able to enter (Fig. 9a and b, yellow arrows) and transfect the human neuroblastoma SH-SY5Y with GFP-cDNA plasmid.

We demonstrated that the amino functionalization has allowed QD-doped NPs to bind DNA (Fig. 7). The ability of 50 nm and 25 nm NPs to enter the cell, carry and release nucleic acids, proved that these nanoparticles can be used as gene delivery tools. Albeit transfection of small antisense oligonucleotide by NH_2–SiO_2 NPs has been already shown [25], our results showed that 50 nm and 25 nm NPs can transfect an entirely exogenous DNA plasmid which will be correctly expressed (Figs. 8 and 9).

4. Conclusion

This work paves the way to the use of NH_2 functionalized CdSe/ZnS QD-doped SiO_2 NPs in the brain. Undoubtedly, a long term toxicological investigation, as well as a deep physiological study focused on the potential signalling impairment of the neurons, will be needed before ultimately validate QD-doped SiO_2 NPs for a potential clinical application. For example, insights regarding NPs interaction with microglia should be deeply investigated in *in vivo* models since the effect of neuroinflammation would be slower than an immediate damage. However, neither behavioral alteration nor brain damage have been seen in our experiments.

The demonstration that amino modified QD-doped silica nanoparticles can be employed as gene carriers for neural cells is very exciting. In the future, it will be attractive to investigate further surface modifications of the NPs in order to reach a specific localization within the body and transfect a selected population of cells.

Acknowledgements

We gratefully acknowledge Rosanna Mastria for CdSe/ZnS QDs synthesis.

Appendix. Supplementary data

Figure 1 Fluorescence microscope images of DIO-C6 (green) stained untreated (a) primary neural cultures; (b) 50 nm red fluorescence emitting CdSe/ZnS QD-doped SiO_2 NPs or (c) 25 nm CdSe/ZnS QD-doped SiO_2 NPs. Nuclei of all cells have been stained with Hoechst 33258. Pictures have been taken after 24 h living cell exposure to nonoparticles.

Figure 2 Phase contrast (a) and Fluorescence microscopy (b) images of primary neural cultures; (c) overlay. Yellow arrows aim at fully differentiated neurons. Flat glia cells are not visible in phase contrast images. Nuclei of all cells have been stained with Hoechst 33258.

Figure 3 Phase contrast (a) and fluorescence confocal microscopy (b) images of primary neural cultures after 15 min in presence of 50 nm NH_2-QD-doped silica NPs.

The supplementary data associated with this article can be found in the on-line version at doi:10.1016/j.biomaterials.2010.04.063.

Appendix

Figures with essential color discrimination. Figs. 5 and 7 in this article are difficult to interpret in black and white. The full color images can be found in the on-line version, at doi:10.1016/j.biomaterials.2010.04.063.

References

[1] Orive G, Anitua E, Pedraz JL, Emerich DF. Biomaterials for promoting brain protection, repair and regeneration. Nat Rev Neurosci 2009;10(9):682–92.
[2] Shvedova AA, Kagan VE, Fadeel B. Close encounters of the small kind: adverse effects of man-made materials interfacing with the nano-cosmos of biological systems. Annu Rev Pharmacol Toxicol;50:63–88.
[3] Fadeel B, Garcia-Bennett AE. Better safe than sorry: understanding the toxicological properties of inorganic nanoparticles manufactured for biomedical applications. Adv Drug Deliv Rev;62(3):362–374.
[4] Jahnen-Dechent W, Simon U. Function follows form: shape complementarity and nanoparticle toxicity. Nanomedicine (Lond) 2008;3(5):601–3.
[5] Schmid G. The relevance of shape and size of Au55 clusters. Chem Soc Rev 2008;37(9):1909–30.
[6] Mayor S, Pagano RE. Pathways of clathrin-independent endocytosis. Nat Rev Mol Cell Biol 2007;8(8):603–12.
[7] Rejman J, Oberle V, Zuhorn IS, Hoekstra D. Size-dependent internalization of particles via the pathways of clathrin- and caveolae-mediated endocytosis. Biochem J 2004;377(Pt 1):159–69.
[8] Chen M, von Mikecz A. Formation of nucleoplasmic protein aggregates impairs nuclear function in response to SiO_2 nanoparticles. Exp Cell Res 2005;305(1):51–62.
[9] Slowing I, Trewyn BG, Lin VS. Effect of surface functionalization of MCM-41-type mesoporous silica nanoparticles on the endocytosis by human cancer cells. J Am Chem Soc 2006;128(46):14792–3.
[10] Chung TH, Wu SH, Yao M, Lu CW, Lin YS, Hung Y, et al. The effect of surface charge on the uptake and biological function of mesoporous silica nanoparticles in 3T3-L1 cells and human mesenchymal stem cells. Biomaterials 2007;28(19):2959–66.
[11] Lin W, Huang YW, Zhou XD, Ma Y. In vitro toxicity of silica nanoparticles in human lung cancer cells. Toxicol Appl Pharmacol 2006;217(3):252–9.
[12] Xing X, He X, Peng J, Wang K, Tan W. Uptake of silica-coated nanoparticles by HeLa cells. J Nanosci Nanotechnol 2005;5(10):1688–93.
[13] Sun W, Fang N, Trewyn BG, Tsunoda M, Slowing II, Lin VS, et al. Endocytosis of a single mesoporous silica nanoparticle into a human lung cancer cell observed by differential interference contrast microscopy. Anal Bioanal Chem 2008;391(6):2119–25.
[14] Trewyn BG, Giri S, Slowing II, Lin VS. Mesoporous silica nanoparticle based controlled release, drug delivery, and biosensor systems. Chem Commun (Camb) 2007;31:3236–45.
[15] Zhao Y, Trewyn BG, Slowing II, Lin VS. Mesoporous silica nanoparticle-based double drug delivery system for glucose-responsive controlled release of insulin and cyclic AMP. J Am Chem Soc 2009;131(24):8398–400.
[16] Chen Z, Chen H, Meng H, Xing G, Gao X, Sun B, et al. Bio-distribution and metabolic paths of silica coated CdSeS quantum dots. Toxicol Appl Pharmacol 2008;230(3):364–71.
[17] Han R, Yu M, Zheng Q, Wang L, Hong Y, Sha Y. A facile synthesis of small-sized, highly photoluminescent, and monodisperse CdSeS QD/SiO(2) for live cell imaging. Langmuir 2009;25(20):12250–5.
[18] Bakalova R, Zhelev Z, Aoki I, Ohba H, Imai Y, Kanno I. Silica-shelled single quantum dot micelles as imaging probes with dual or multimodality. Anal Chem 2006;78(16):5925–32.
[19] Bottini M, D'Annibale F, Magrini A, Cerignoli F, Arimura Y, Dawson MI, et al. Quantum dot-doped silica nanoparticles as probes for targeting of T-lymphocytes. Int J Nanomedicine 2007;2(2):227–33.

[20] Dabbousi BO, Rodriguez-Viejo J, Mikulec FV, Heine JR, Mattoussi H, Ober R, et al. (CdSe)ZnS core-shell quantum dots: synthesis and characterization of a size series of highly luminescent nanocrystallites. J Phys Chem B 1997;101:9463–75.
[21] Peng ZA, Peng X. Formation of high-quality CdTe, CdSe, and CdS nanocrystals using CdO as precursor. J Am Chem Soc 2001;123(1):183–4.
[22] Bardi G, Tognini P, Ciofani G, Raffa V, Costa M, Pizzorusso T. Pluronic-coated carbon nanotubes do not induce degeneration of cortical neurons in vivo and in vitro. Nanomedicine 2009;5(1):96–104.
[23] Harry GJ, Billingsley M, Bruinink A, Campbell IL, Classen W, Dorman DC, et al. In vitro techniques for the assessment of neurotoxicity. Environ Health Perspect 1998;106(Suppl. 1):131–58.
[24] Chang JS, Chang KL, Hwang DF, Kong ZL. In vitro cytotoxicitiy of silica nanoparticles at high concentrations strongly depends on the metabolic activity type of the cell line. Environ Sci Technol 2007;41(6):2064–8.
[25] Peng J, He X, Wang K, Tan W, Li H, Xing X, et al. An antisense oligonucleotide carrier based on amino silica nanoparticles for antisense inhibition of cancer cells. Nanomedicine 2006;2(2):113–20.